



HAL
open science

AMONG SPACE FUNDAMENTAL PHYSICS MISSIONS, MICROSCOPE, A SIMPLE CHALLENGING FREE FALL TEST

Pierre Touboul, Ratana Chhun, Damien Boulanger, Manuel Rodrigues, Gilles
Metris

► **To cite this version:**

Pierre Touboul, Ratana Chhun, Damien Boulanger, Manuel Rodrigues, Gilles Metris. AMONG SPACE FUNDAMENTAL PHYSICS MISSIONS, MICROSCOPE, A SIMPLE CHALLENGING FREE FALL TEST. 46th Rencontres de Moriond on Gravitational Waves and Experimental Gravity, Mar 2011, La Thuile, Italy. hal-04417677

HAL Id: hal-04417677

<https://hal.science/hal-04417677>

Submitted on 25 Jan 2024

HAL is a multi-disciplinary open access archive for the deposit and dissemination of scientific research documents, whether they are published or not. The documents may come from teaching and research institutions in France or abroad, or from public or private research centers.

L'archive ouverte pluridisciplinaire **HAL**, est destinée au dépôt et à la diffusion de documents scientifiques de niveau recherche, publiés ou non, émanant des établissements d'enseignement et de recherche français ou étrangers, des laboratoires publics ou privés.

AMONG SPACE FUNDAMENTAL PHYSICS MISSIONS, MICROSCOPE, A SIMPLE CHALLENGING FREE FALL TEST

P. TOUBOUL¹, R. CHHUN¹, D. BOULANGER¹,
M. RODRIGUES¹, G. METRIS²

¹*Onera, The French Aerospace Lab, Chemin de la Hunière, 91761 Palaiseau Cedex, France*

²*Observatoire de la Côte d'Azur, GeoAzur, Grasse, France.*

Several space tests of gravity laws have already been performed but the MICROSCOPE mission is the first one to be fully dedicated to the test of the Equivalence Principle. The dedicated payload is now under qualification and the rather large micro satellite will be produced by Cnes for a launch at beginning of 2015. Each of the two differential accelerometers of the experimental device includes a pair of test-masses whose 720 km altitude orbital motions are constrained along the same purely gravitational trajectory. Evidence of an EP violation is provided by the comparison of the electrostatic configurations needed to maintain the two masses composed of different materials motionless relative to each other. Not only the servo-loop electronics must exhibit very weak level of noise but the geometrical and electrical configuration of the instruments must be very well optimised, accurate, cleaned and steady. Although the accelerometers are saturated on ground by normal gravity, they can be tested on board a free fall capsule in drop tower. These tests complete the fine verification of all mechanical and electrical functions. In addition, the present in flight results of the GOCE mission accelerometers are deeply analysed. Because the sensors of the gravity gradiometer exploits the same technologies, they provide confirmation of the MICROSCOPE instrument models used to extrapolate the in orbit performance and then estimate the expected mission accuracy.

1. The MICROSCOPE space mission

One century after Einstein¹'s paper on special relativity, initiating his elaboration of the new formulation of gravitational interactions, space remains the favorite environment to perform deep experimental investigation on Gravitation. After the Pound and Rebka² experiments in 1959, demonstrating frequency red shift with γ rays emission, R. Vessot³ has performed in 1976 the comparison of two clocks at different gravity potential taking advantage of the parabolic trajectory of a rocket, up to an altitude of ten thousand kilometers. With this Gravity Probe A mission, redshift of 4.10^{-10} was measured with clock frequency stability of 10^{-14} . The ACES (Atomic Clock Ensemble in Space) payload will be accommodated in 2014 on board the International Space Station and will include Hydrogen Maser and the cold atom PHARAO clock with a fine microwave link in order to perform, among other metrological objectives like C isotropy, time dilatation or time distribution, the comparison with ground clocks with an expected accuracy better than 10^{-16} [L. Cacciapuoti⁴].

The three ton Gravity Probe B satellite was launched in April 2004 for 18 month operating mission. The drag free satellite mainly carries four dedicated cryogenic gyros in a very steady configuration, aligned with an inertially pointed telescope, in order to perform the accurate measurement of both the geodetic and the frame dragging effect along the Earth polar circular orbit at an altitude of 642 km. With a specific data processing, developed to correct the limitation of the gyros, induced by unforeseen electrical anisotropic charging of their spherical rotor and cage, the expected -6606.1 milliarcsecond/year N-S geodetic drift was measured with 0.3 % accuracy

(-6601.8 \pm 18.3 mas/yr) and the -39.2 mas/yr frame dragging drift with 20 % accuracy (-37.2 \pm 7.2 mas/yr) [C.W.F. Everitt ⁵]. These results agree with the previously measured Lense-Thirring effect on satellite orbital plane, previously performed with the LAGEOS 2 satellite. Eleven years of fine laser tracking of the 5620 km altitude orbit have been revisited taking advantage of the more accurate Earth gravity field model obtained from the GRACE space mission data. 10 % uncertainty on the measured effect was then evaluated by I. Ciufolini ⁶.

The Parameterized Post-Newtonian (PPN) formalism is often considered to interpret the space tests of general relativity and γ and β are presently respectively limited to the following ranges:

- $\gamma-1 = 2.1 \pm 2.3 \cdot 10^{-5}$, as computed by B. Bertotti et al. ⁷ from the Cassini spacecraft navigation during its cruise from Jupiter to Saturn with the solar conjunction between Earth and Satellite,
- $\beta-1 = 1.2 \pm 1.1 \cdot 10^{-4}$, as deduced by J.G. Williams et al. ⁸ from the accurate measurements by lunar laser ranging, of the relative motions of the Earth and Moon in Solar gravity field.

Other space tests of gravity are now proposed. Among them, the Outer Solar System mission proposed by B. Christophe et al. ⁹ envisages long range gravity test by finely tracking the gravitational motion of an interplanetary spacecraft carrying an electrostatic ultra-sensitive accelerometer to permanently survey any deviation from geodesic motion. The SAGAS mission, proposed by P. Wolf et al. ¹⁰ is much more ambitious considering a large satellite, able to cross the solar system with an optical atomic clock on board, cold atom interferometers as accelerometers and gyrometers, laser links for the satellite motion tracking with many major objectives like the test of universal redshift, the test of Lorentz invariance, PPN test, large scale gravity, variation of cosmologic constant...

For what concerns the MICROSCOPE mission, it is fully dedicated to the test of the Equivalence Principle (EP). It has been selected by Cnes in 2004, the instrument is now under qualification and the satellite production should start this year for a launch of the satellite in 2015.

The accurate test of the universality of free fall represents today much more than the verification of this well known property. The violation of the universality of free fall leads to the violation of the Equivalence Principle (EP), fundamental basis of the Einstein General Relativity. Einstein, himself, considered this symmetry as enacted by the experience. Today, most attempts of Grand Unification like String theory and M-theory allow the violation of this principle, introducing in particular scalar fields ¹¹, while the experimental investigation of quantum gravity does appear directly very weakly accessible. The test of the Equivalence Principle is thus not only the test of general relativity but also the search for new experimental results as the necessary support for new theories: as expressed by T. Damour ¹², EP test appears much more relevant by about a factor 10^6 than γ accurate determination when comparing presently obtained γ and EP test accuracy. In addition, Super symmetry might be confirmed by the CERN LHC near future results with new particles to be taken into account. The test of the universality of free fall with ultimate accuracy is then an important challenge and has also to be considered regarding dark matter query.

Present laboratory tests, performed by the Eötvash group ¹³ reached a few 10^{-13} accuracy: the dedicated torsion pendulum exploits the 1m long, 20 μ m diameter tungsten fibre, exhibiting a Q factor of about 5000. It is surrounded with 800 kg of lead designed to compensate the local gravity gradients. Much care is also taken to reject the vibrating environment and the thermal effects. The data can be integrated over periods as long as 3 months.

MICROSCOPE space experiment has been designed and the payload and the satellite specified to obtain at least two orders of magnitude better, i.e. 10^{-15} accuracy. Other missions are also proposed by A. Nobili ¹⁴ or T. Sumner ¹⁵ to perform this test with outstanding accuracy of 10^{-17} or 10^{-18} . But not only the instruments demand new long developments but such missions require quite 10 times heavier satellites with much demanding performance for attitude controls and drag free motions as well as for the experiment environment controls.

2. The MICROSCOPE experiment

The MICROSCOPE satellite is rather small, 270 kg in its definitive definition, with its new cold gas propulsion system, leading to major constraints on the dedicated scientific payload available mass, volume and power, respectively, 35 kg, 40 cm³ and 40 W, leading to a non cryogenic experiment, with

a limited couple of tested materials. The test performance relies on available technologies for the instrument and the satellite. Even better performance could be reached in the future but with more complex satellite, instrument and operation.

The MICROSCOPE space experiment consists in a basic free-fall test of two masses around the Earth, with the availability of long duration of measurement, reduced test-mass disturbing accelerations, very precise instruments optimized for micro-gravity operation and modulation of the Earth gravity signal by rotation of the satellite and the instrument axis along the orbit.

The two test masses made of different composition will be precisely positioned on the same orbit and so submitted to the same Earth gravity field. In absence of Equivalence Principle violation, the two masses will continue on the same common trajectory. The MICROSCOPE satellite, protecting them from Earth and Sun radiation pressures and from residual atmospheric drag, will be controlled to follow the common trajectory of the masses by acting the thrusters of its propulsion system. In fact, the relative motion of both masses with respect to the instrument frame will be accurately measured and servo-controlled thanks to generated electrical field around the conductive masses. The masses are then maintained motionless with respect to the instrument parts to an accuracy better than 10^{-11} m, insuring the stability of the configuration and thus limiting the fluctuations of the eventual disturbing forces acting on them: gravity field gradients, electro-magnetic field, patch effects...Such protocol permits to linearize the position capacitive sensing and the electrostatic actuations, mainly depending on the configuration geometry. The electrostatic acceleration generated commonly on the two masses is nullified by acting the satellite thrusters in such a way that the common instrument reference frame follows the two masses in their orbital motion. The difference of the applied electrostatic acceleration is accurately measured and the projection along the Earth gravity monopole is analysed as an eventual Equivalence Principle violation signal.

The masses are almost perfectly cylindrical and concentric¹⁶. Each one is surrounded by two gold coated silica rods which carry electrodes for position sensing and electrical field servo-control. Rods and test mass, associated to six electronics channels for the control of the six degrees of freedom of the mass constitute a six-axis ultra-sensitive inertial sensor [P. Touboul et al.¹⁷]. The two concentric inertial sensors compose the SAGE instrument (Space Accelerometer for Gravitational Experimentation). The MICROSCOPE satellite can operate two SAGE instruments that will be identical except for the mass materials. The two materials used for the test will be Platinum Rhodium alloy, PtRh10 (90% Pt, 10% Rh), and Titanium alloy, TA6V (90% Ti, 6% Al, 4% Va), respectively 402.336 g and 300.939 g. The two other masses are made of same Pt-Rh alloy, respectively 402.336 g and 1361.230 g measured on masses manufactured by PTB in Braunschweig, as qualification parts. This second instrument is only devoted to the in orbit verification of the systematic experiment errors. The experiment then consists in a double differentiation. The Pt-Rh alloy has been selected for its high density, leading to a better rejection of the spurious surface effects: better performance is expected with the two same material test masses insuring the confidence in the obtained EP test result.

The MICROSCOPE satellite is scheduled to be launched in 2015 along a quasi-circular heliosynchronous orbit at an altitude of 720 km. The heliosynchronism allows a fixed satellite Sun side and optimised AsGa rigid solar panels with maximum delivered power and minimum sizes to reduce the radiation pressure and the atmospheric drag. Furthermore, the thermal external conditions are steady and thus very favourable for its thermo-elastic behaviour and its internal fluctuations of temperature. 1mK stability at orbital frequency has been demonstrated by Cnes with the thermal representative model of the instrument accommodated inside its satellite cocoon. The electronics units are stabilized at 10 mK and the external anti-Sun radiator is protected against the Earth albedo to exhibit a steady temperature. The propulsion system consists in two symmetric assemblies accommodated on two faces of the cubic satellite, each one comprising 3 Nitrogen tanks (8,25 kg, 345 bars), servo-valves and command electronics to 4 pods of two thrusters. The continuous and proportional actuation of the thrusters allows fine control of the satellite motion. The satellite positioning must be a posteriori known at the EP orbital frequency with 7 m accuracy radially and 14 m along track, and the inertial pointing with 6 μ rad in such a way that the Earth gravity gradient can be rejected. When the satellite is rotating, the specification is even more stringent: 1 μ rad. In addition, the satellite linear and angular acceleration fluctuations are controlled to be respectively less

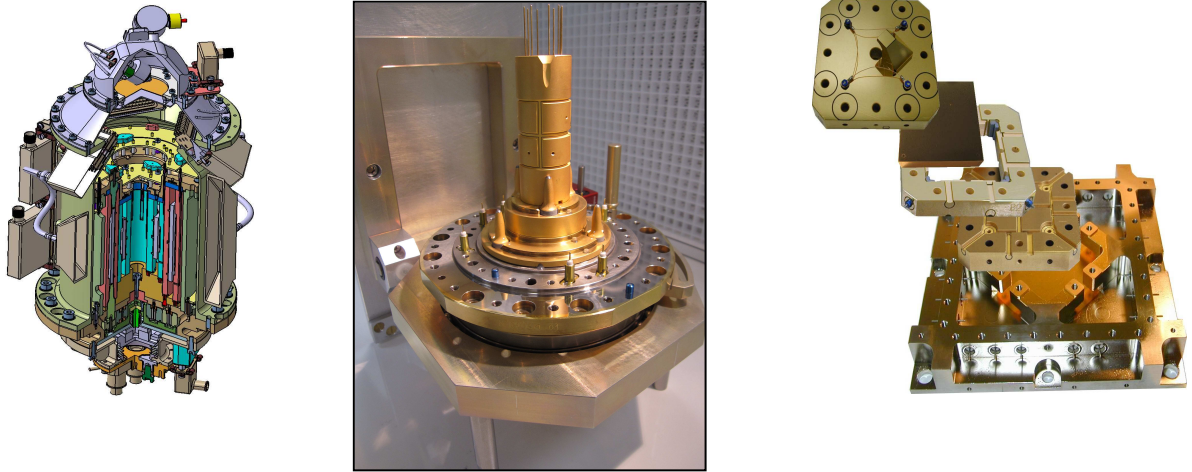


Figure 1: Comparison of MICROSCOPE and GOCE sensor configuration. The parallelepiped GOCE mass is surrounded by three planar gold coated electrode plates (*right*). The cylindrical configuration of MICROSCOPE includes also 4 quadrant pairs of electrodes for the control of the 2 radial directions, translation and rotation (*left*).

than $3 \cdot 10^{-10} \text{ ms}^{-2}/\text{Hz}^{1/2}$ and $5 \cdot 10^{-9} \text{ rds}^{-2}/\text{Hz}^{1/2}$ about the EP frequency. This is performed by finely servo-acting the thrusters according to the instrument measurements themselves.

The one year mission includes different instrument calibration and measurement sequences. The symmetry of the electrostatic actuations, the scale factors of the measurement pickup, the alignments of the measurement axes are calibrated in orbit to 10^{-4} relative accuracy in order to reject at same level common motion disturbances [V. Josselin et al. ¹⁸]. The off-centring of the masses, less than $20 \mu\text{m}$ after instrument integration, is also evaluated to $0.1 \mu\text{m}$ accuracy in the orbital plane and $0.2 \mu\text{m}$ normal to the orbit, in order to sufficiently correct the gravity gradient disturbances. Several EP test experiments are performed between calibration sessions with inertial and rotating pointing (at two different frequencies) of the satellite. In case of inertial pointing, the EP test is performed at the orbital frequency, *i.e.* $f_{\text{EPi}} = 1.7 \times 10^{-4} \text{ Hz}$. In rotating pointing, the test is performed at the sum of the orbital frequency plus the satellite spin rate, *i.e.* $f_{\text{EPs}} = \text{about } 10^{-3} \text{ Hz}$. This is the modulation frequency of the Earth gravity along the axial direction of the instrument. Sessions of 20 orbits are processed to reject the stochastic errors.

3. MICROSCOPE and GOCE instruments

The four MICROSCOPE inertial sensors take advantage of the same concept and technologies already used for the GOCE gradiometer sensors ¹⁹. In the ESA GOCE mission, the gravity gradiometer is composed of six accelerometers mounted in a diamond configuration corresponding to 3 identical orthogonal gradiometer of 50 cm arm ²⁰. The satellite was launched on March 17th of 2009 and injected in a very low heliosynchronous orbit at altitude of 260 km. Three diagonal components of the Earth gravity gradient can be deduced from the difference of the outputs provided by each pair of aligned sensors.

As in MICROSCOPE, each proof-mass of each sensor is electrostatically levitated at the centre of the instrument silica cage without any mechanical contact except a thin $5 \mu\text{m}$ diameter gold wire to manage the mass global charge against the space high energy proton fluxes bombarding the satellite and creating also secondary electrons (see Figure 1) ²¹.

Surrounded by electrodes and electrical shield engraved in silica or glass ceramic gold coated parts, the mass is naturally unstable because of the attractivity of the electrostatic forces. So, six channels, including digital controllers, generate, from the data provided by six capacitive position sensors (motion and attitude), opposite electrical voltages. These voltages are applied on related electrodes, used for both capacitive sensing and electrostatic actuation, opposite versus the mass whose electrical potential is biased. Cold damping of all degrees of motion is provided in addition to a very accurate

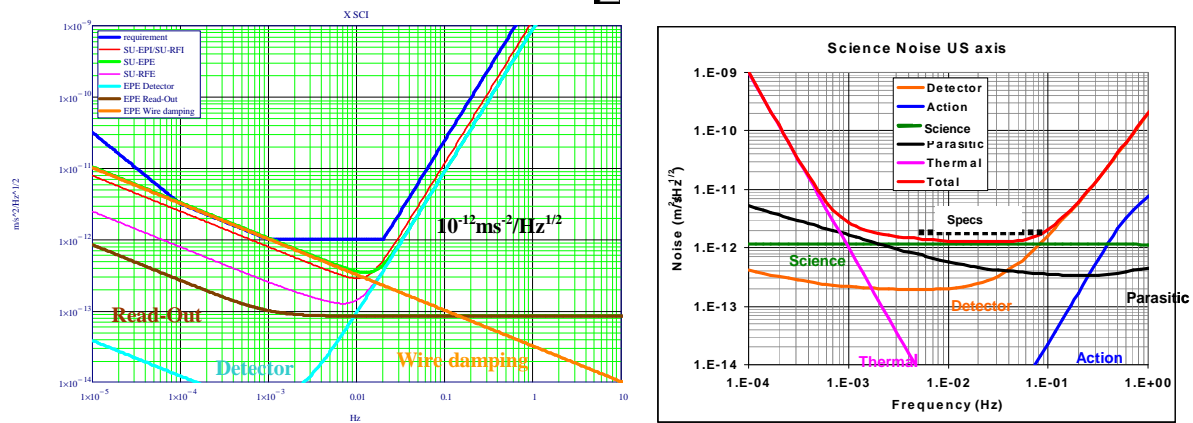


Figure 2: Comparison of MICROSCOPE (left) and GOCE (right) stochastic errors: $\sqrt{\text{PSD}}$ expressed in $\text{ms}^{-2}\text{Hz}^{1/2}$. Models depend on configuration, electronics performance, thermal stabilities and environment conditions.

mass positioning. The accurate measurements of the applied electrostatic forces and torques provide the data for the satellite pointing and for the drag compensation as well as for the scientific outputs.

Figure 2 compares computed power spectral density of both MICROSCOPE and GOCE stochastic acceleration errors in the instrument frequency bandwidth. Major error sources are the following from upper frequencies to lower: capacitive sensor noise, analogue to digital data conversion, disturbing mass motion forces and in particular gold wire damping, thermal instabilities of the geometrical and electrical configurations.

The GOCE sensor is optimized for the frequency bandwidth from 5.10^{-3} Hz to 0.1 Hz, corresponding to the fine recovery of the Earth gravity potential harmonics between orders 25 and 500. MICROSCOPE is optimised for lower frequencies, from orbital frequency of $1.7 \cdot 10^{-4}$ Hz to calibration frequencies of a few 10^{-3} Hz.

The resolutions presented in Table 1 are obtained along the axial direction of each sensor, with a full measurement range of $\pm 2.5 \cdot 10^{-7} \text{ ms}^{-2}$ and the saturation of the electrostatic control larger than 10^{-6} ms^{-2} . GOCE sensor full range is larger, $\pm 6.5 \cdot 10^{-6} \text{ ms}^{-2}$, requiring smaller gaps between the mass and the electrodes, 299 μm instead of 600 μm but increasing the electrical defects due to contact potential differences²² or thermal sensitivity because of the mass coefficient of thermal expansion versus the quite null silica one.

From the switch on of the GOCE sensors, in April 2009, the operation of the GOCE sensors has been finely verified and tested in orbit through different calibration sequences and by the redundancy of the provided measurements. Each sensor provides six outputs depending on the residual satellite drag, the gravity gradient and the angular and centrifugal acceleration. The drag compensation of the satellite, performed by exploiting the accelerometer outputs, has been verified down to a level of $10^{-9} \text{ ms}^{-2}/\text{Hz}^{1/2}$, ten times better than required. And the observed sensor noise PSD has confirmed our model of the respective electronics noise contributions, through the servo-loops, of the position sensing and the electrostatic actuation²³.

One invariant in the GOCE mission data is the measured trace of the Earth gravity gradient that should be null in absence mainly of accelerometer noise, in flight calibration inaccuracy and centrifugal acceleration residue. Present analysis leads to flat noise of each gradiometer axis output in the frequency bandwidth from 5.10^{-2} Hz to 0.1 Hz: 11 $\text{mE}/\text{Hz}^{1/2}$ along track (x), 9 $\text{mE}/\text{Hz}^{1/2}$ normal to the orbit (y) and 19 $\text{mE}/\text{Hz}^{1/2}$ in the radial direction (z). And the residue in the trace is $24 \text{ mE}/\text{Hz}^{1/2}$.

By considering that all residual noises are only due to the six sensors, this leads to $4.9 \cdot 10^{-12} \text{ ms}^{-2}/\text{Hz}^{1/2}$ and more precisely for the pairs of each axis: $3.9 \cdot 10^{-12} \text{ ms}^{-2}/\text{Hz}^{1/2}$ for both sensors along x, $3.1 \cdot 10^{-12} \text{ ms}^{-2}/\text{Hz}^{1/2}$ along y and $6.7 \cdot 10^{-12} \text{ ms}^{-2}/\text{Hz}^{1/2}$ along z. Because all six sensors are identical, it is reasonable to consider that their contribution is limited to less than $3.1 \cdot 10^{-12} \text{ ms}^{-2}/\text{Hz}^{1/2}$,

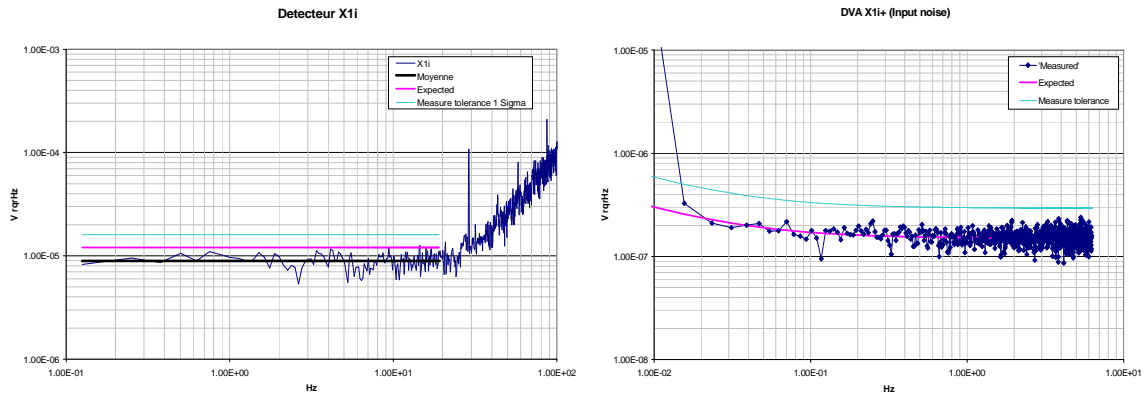


Figure 3: MICROSCOPE capacitive sensor output noise, $10\mu\text{V}/\text{Hz}^{1/2}$ flat level (left) and actuator input noise (right), $0.15\mu\text{V}/\text{Hz}^{1/2}$ flat level

to be compared to the MICROSCOPE sensor stochastic error specification including not only the intrinsic noise but also the effect of the thermal environment fluctuations, i.e. $3.3 \cdot 10^{-12} \text{ms}^{-2}/\text{Hz}^{1/2}$ in inertial pointing and $1.4 \cdot 10^{-12} \text{ms}^{-2}/\text{Hz}^{1/2}$ in rotating mode.

Dedicated in orbit tests of the GOCE sensors have been also performed by opening the electrostatic loops and observing the electronics outputs while the mass is resting gently on its mechanical stops: this has confirmed the expected electronics contribution of the analogue to digital conversion in particular²⁴. By applying in the electrostatic loops biasing position signals, it has also been possible to move the mass in its cage and deduce any unexpected stiffness or non linear behaviour. In addition this has confirmed the operation model assessing the MICROSCOPE sensor error budget derived from the same formulas.

At last, because of the redundancy of two pairs of electrodes to only control the z axis motion of the parallelepiped mass, it is possible to compare two outputs and deduce a $5\mu\text{V}/\text{Hz}^{1/2}$ residue that is not yet well explained. Nevertheless, such electrical voltage fluctuations applied on the MICROSCOPE sensor electrodes lead to $0.53 \cdot 10^{-13} \text{ms}^{-2}/\text{Hz}^{1/2}$ for the PtRh inner mass and $0.23 \cdot 10^{-12} \text{ms}^{-2}/\text{Hz}^{1/2}$ for the TA6V outer mass, which is compatible with MICROSCOPE specifications.

4. Present instrument and tests status, perspectives

In parallel to the satellite and mission definitions, models of the instrument have been developed and tested. The flight models of the analogue functional electronics units have been carefully tested and exhibit very weak noise. The capacitive sensor noise is at lower frequencies than 10 Hz around $10 \mu\text{V}/\text{Hz}^{1/2}$ (see Figure 3). According to the capacitive sensor sensitivity and the geometry, the position resolution is deduced (see Table 2).

These position resolutions corresponds to less than $6.10^{-17} \text{ms}^{-2}$ for the highest EP frequency when integrated over 20 orbits with a back action of the sensor signals limited to less than $3.10^{-17} \text{ms}^{-2}$ when expressed in acceleration. In addition the thermal sensitivities of the sensor biases are respectively measured to $71\mu\text{V}/^\circ\text{C}$ and $12\mu\text{V}/^\circ\text{C}$, corresponding to $24.10^{-1} \text{m}/^\circ\text{C}$ and $4.5 \cdot 10^{-1} \text{m}/^\circ\text{C}$, in agreement to the demonstrated thermal stability of 10^{-2}°C .

Furthermore, the qualification model of the double inertial sensor instrument, integrating two PtRh masses, has been produced and integrated according to the established procedures for the flight models. This model integrates very accurate test masses and silica parts as well as the blocking mechanism which is used to clamp the masses during launch vibrations. Environmental tests have been performed as well as tests of the instrument operation in micro-gravity. These tests, realized in the ZARM drop tower in Bremen, have allowed optimising the twelve control laws of both masses electrostatic levitation. In spite of the limited duration of the fall, 4.7 s, the convergence of the mass position has been compared to the established models in order to fix the digital recursive filters that will be implemented in the interface and control unit of the experiment.

Table 1: MICROSCOPE inertial sensors computed performances in steady environment deduced from the test of the flight model electronics units and from the characteristics of the qualification models of the sensor; satellite rotation frequency = $(\pi + 1/2)$ orbital frequency (a) or $(\pi + 3/2)$ orbital frequency (b)

| Pointing | Inner PtRh mass $\text{ms}^{-2}/\text{Hz}^{1/2}$ | Outer TA6V mass $\text{ms}^{-2}/\text{Hz}^{1/2}$ |
|---|---|---|
| Inertial $f_{\text{EP}} = 1.7 \cdot 10^{-4} \text{ Hz}$ | $1.92 \cdot 10^{-12}$ | $2.55 \cdot 10^{-12}$ |
| Rotating ^a $f_{\text{EP}} = 7.8 \cdot 10^{-4} \text{ Hz}$ | $0.89 \cdot 10^{-12}$ | $1.18 \cdot 10^{-12}$ |
| Rotating ^b $f_{\text{EP}} = 9.5 \cdot 10^{-4} \text{ Hz}$ | $0.81 \cdot 10^{-12}$ | $1.07 \cdot 10^{-12}$ |

Table 2: MICROSCOPE test-mass position resolution deduced from capacitive sensor electronic noise and sensitivity as well as from the geometry of the electrical conductors

| | Capacitive sensor gain in V/pF | Electronic noise in $\text{pF}/\text{Hz}^{1/2}$ | Capacitive variation vs. mass displacement in $\text{pF}/\mu\text{m}$ | Capacitive sensor gain in $\text{V}/\mu\text{m}$ | Position sensor resolution in $\text{m}/\text{Hz}^{1/2}$ |
|-----------------|---|--|--|---|---|
| PtRh inner mass | 80 | $1.25 \cdot 10^{-7}$ | 3.7 | 0.30 | $4.0 \cdot 10^{-11}$ |
| TA6V outer mass | 40 | $2.5 \cdot 10^{-7}$ | 6.5 | 0.26 | $3.8 \cdot 10^{-11}$ |

The qualification of the instrument gives also the latest data to update the instrument and mission error budgets taking into account the expected performance of the satellite sub-systems as defined now. The four major stochastic errors are the following:

- the mass damping induced by the gold wire,
- the radiometer pressure on the mass taking into account the thermal gradient in the instrument tight housing,
- the satellite centrifugal acceleration combined to the mass off-centring,
- the angular acceleration residue combined to the mass off-centring,

leading to a total amount of $1.5 \cdot 10^{-12} \text{ ms}^{-2}/\text{Hz}^{1/2}$.

The four major systematic error sources are at the f_{EP} frequency:

- the instability of the star tracker with respect to the instrument measurement axes,
- the drag free residual acceleration when considering the 10^{-4} sensitivity and alignment matching,
- the magnetic field taking into account the rejection by the instrument magnetic shield and the masses susceptibilities,
- and the satellite angular acceleration residue combined to the mass off-centring,

leading to a total amount of $1.1 \cdot 10^{-15} \text{ ms}^{-2}$ tone error at the f_{EP} frequency.

This corresponds, in satellite rotating mode, to the expected EP test accuracy of $6 \cdot 10^{-16}$ with 20 orbit signal integration. Tens of 20 orbit measurement sequences are foreseen in the mission scenario. Next step in the mission development will be the satellite production and qualification. The instrument flight models should be delivered in 2012, to be integrated in 2013, for a launch in 2015.

Acknowledgments

The authors would like to thank ONERA and CNES for their financial support and the respective MICROSCOPE and CNES teams for the technical exchanges as well as Bruno Christophe and Bernard Foulon for the fruitful discussions.

References

1. A. Einstein, *Annalen der Physik*, **17** (1905)
2. R.V. Pound and G.A. Rebka *Phys. Rev. Lett.*, **3**, 439–441 (1959)
3. R.F.C. Vessot et al., *Phys. Rev. Lett.*, **45**, 2081-2084 (1980)
4. L. Cacciapuoti and C. Salomon, *EPJ*, **172**, 57 (2009)
5. C.W.F. Everitt et al, *Phys. Rev. Lett.*, **106**, 221101, (2011)
6. I. Ciufolini and E.C. Pavlis, *NATURE*, **431**, 7011, 958-960 (2004)
7. B. Bertotti, L. Iess, P. Tortora, *Nature*, **425**, 374-376 (2003)
8. J.G. Williams, S.G. Turyshev, D.H. Boggs, *Phys. Rev. Lett.*, **93**, 261101 (2004)
9. B. Christophe et al, *Exp. Astron.*, **23**, 529-547 (2009)
10. P. Wolf et al, *Exp. Astron.*, **23**, 651-687 (2009)
11. T. Damour and M. Lilley, arXiv:0802.4169v1 [hep-th] (2008)
12. T. Damour and J.F. Donoghue, arXiv:1007.2792v2 [gr-qc] (2010)
13. S. Schlamminger et al, *Phys. Rev. Lett.*, **100**, 041101 (2008)
14. A.M. Nobili et al, *Adv. Space Res.*, **25**, 6, 1231-1235 (2000)
15. T. Sumner et al, *Adv. Space Res.*, **39**, 254-258, (2007)
16. R. Chhun et al., *IAU symposium proceedings*, **261**, 402-408 (2009)
17. P. Touboul, *ISSI Space Science Series*, **34**, Springer (2010)
18. V. Josselin et al, *Space Sciences Review*, **151**, 25-38 (2010)
19. P. Touboul et al., *Aerospace Science and Technology*, **8**, **5**, 431-441 (2004)
20. J.P. Marque et al, IAC-08-B1.3.7 (2010)
21. P. Touboul et al., *Acta Astronautica*, **45**, **10**, 605-617 (1999)
22. C.C. Speake, *Class. Quantum Grav.*, **13**, A291-A297 (1996)
23. P. Touboul et al, *Series Proceedings IAG Symposia*, **136**, Sneeuw Ed. (2011)
24. B. Christophe et al., *SF2A Meeting Proceedings*, 113 (2010)